Poly(triphenylamine)s Derived from Oxidative Coupling Reaction: Substituent Effects on the Polymerization, Electrochemical, and Electro-Optical Properties

HUNG-YI LIN,[1] GUEY-SHENG LIOU[2]

[1]Department of Applied Chemistry, National Chi Nan University, 1 University Rd. Puli, Nantou Hsien 54561, Taiwan

[2]Institute of Polymer Science and Engineering, National Taiwan University, No.1, Sec. 4, Roosevelt Rd. Taipei 10617, Taiwan

Received 19 September 2008; accepted 11 October 2008
DOI: 10.1002/pola.23155
Published online in Wiley InterScience (www.interscience.wiley.com).

ABSTRACT: A series of triphenylamine-based polymers containing electron-donating methoxy (—OCH_3) and electron-withdrawing cyano or nitro (—CN or —NO_2) substituents in the main chains have been designed and investigated. These conjugated polymers (**P1**–**P3**) could be readily prepared by oxidative coupling polymerization from monomers (**M1**–**M3**) using $FeCl_3$ as an oxidant. The **P2** and **P3** exhibited moderate high T_g values (203–205 °C) and thermal stability. These polymers in NMP solution showed UV–vis absorption around 288–404 nm and photoluminescence peaks around 435–492 nm. **P1**–**P3** showed reversible oxidation redox couples at E_{onset} = 0.67, 0.99, and 1.00 V in solution of 0.1 M tetrabutylammonium perchlorate (TBAP)/acetonitrile (CH_3CN), respectively. **M3** and **P3** exhibited reversible reduction redox couples at E_{onset} = −1.04 and −1.03 V. These polymers also revealed electrochromic characteristic changing color at different potential. © 2008 Wiley Periodicals, Inc. J Polym Sci Part A: Polym Chem 47: 285–294, 2009

Keywords: conjugated polymers; electrochemistry; fluorescence; functionalization of polymers; high-performance polymers

INTRODUCTION

In the past decade, conjugated polymers have received considerable attention because of their promising applications in optic-electronic devices,[1,2] such as electroluminescence display,[3] thin film transistor,[4] and photovoltaic devices.[5,6] In particular, significant progress has been achieved in the development of light-emitting diodes (LEDs) based on conjugated polymer.[7,8] Triarylamines have attracted considerable interest as hole-transport materials for using in multilayer organic electroluminescence (EL) devices because of their relatively high mobility and their low ionization potentials.[9–12] The characteristic structure feature of triphenylamine (TPA) is the electroactive nitrogen atom, which is linked to three electron-rich phenyl groups in a propeller-like geometry. The anodic oxidation of TPA in aprotic solvent was well studied in 1966.[13] The electrogenerated cation radical of TPA^+ is not stable and could to form tetraphenylbenzidine (TPB) by tail-to-tail coupling. TPB is more easily oxidized than the TPA molecule. When the phenyl groups are substituted by electron-donating groups at the

Additional Supporting Information may be found in the online version of this article.

Correspondence to: G.-S. Liou (E-mail: gsliou@ntu.edu.tw)

Journal of Polymer Science: Part A: Polymer Chemistry, Vol. 47, 285–294 (2009)

para-position, the couple reactions could be greatly prevented by giving stable cation radicals.[14]

To obtain high T_g hole-transporting polymers, many research groups have prepared polymers containing TPA units in the main and/or chain,[15–23] such as Ogino and Kakimoto.[24–27] Recently, we have reported the synthesis of soluble aromatic polyamides and polyimides bearing TPA units in the main chain.[28–35] Because of the incorporation of bulky and three-dimensional TPA units along the polymer backbone, all the polymers were amorphous and soluble in many organic solvents with excellent thin film formability. Polymeric triarylamines are prepared using copper-mediated Ullman reactions,[36] palladium[37,38] or nickel-catalyzed coupling reactions,[39,40] and nucleophilic substitution reactions.[41] However, these synthetic methods are not straightforward and require multiple steps to prepare the monomers. Therefore, we need a simple and rapid method to replace the aforementioned reaction. Herein, we design a series of different para-substituted TPA-based homopolymers (Scheme 1) by using $FeCl_3$ as an oxidant and report the synthesis, characteristics, photophysical, electrochemical properties, and the substituent effect for the coupling reaction.[42]

EXPERIMENTAL

Materials

Diphenylamine (99%, ACROS), 4-fluorobenzonitrile (99%, TCI), 4-fluoronitrobenzene (99%, ACROS), 4-iodoanisole (98%, ALFA AESAR), sodium hydride (95%, Aldrich), copper powder (99% ACROS), potassium carbonate (SCHARLAU), triethyleneglycol dimethyl ether (TEGDME) (99%, ALFA AESAR), iron (III) chloride (SHOWA), toluene (TEDIA), nitrobenzene (ACROS), *N,N*-dimethylacetamide (DMAc) (TEDIA), *N,N*-dimethylformamide (DMF) (ACROS), *N*-methyl-2-pyrrolidinone (NMP) (TEDIA), chloroform ($CHCl_3$) (TEDIA), and tetrahydrofuran (THF) (ECHO) were used without further purification. Tetrabutylammonium perchlorate (TBAP) was obtained from ACROS and recrystallized twice from ethyl acetate and then dried *in vacuo* prior to use. All other reagents were used as received from commercial sources.

Monomer Synthesis

M1 and **M3** synthesis routes according to the previous literature.[43,44] **M1** (Mp: 108–110 °C) was

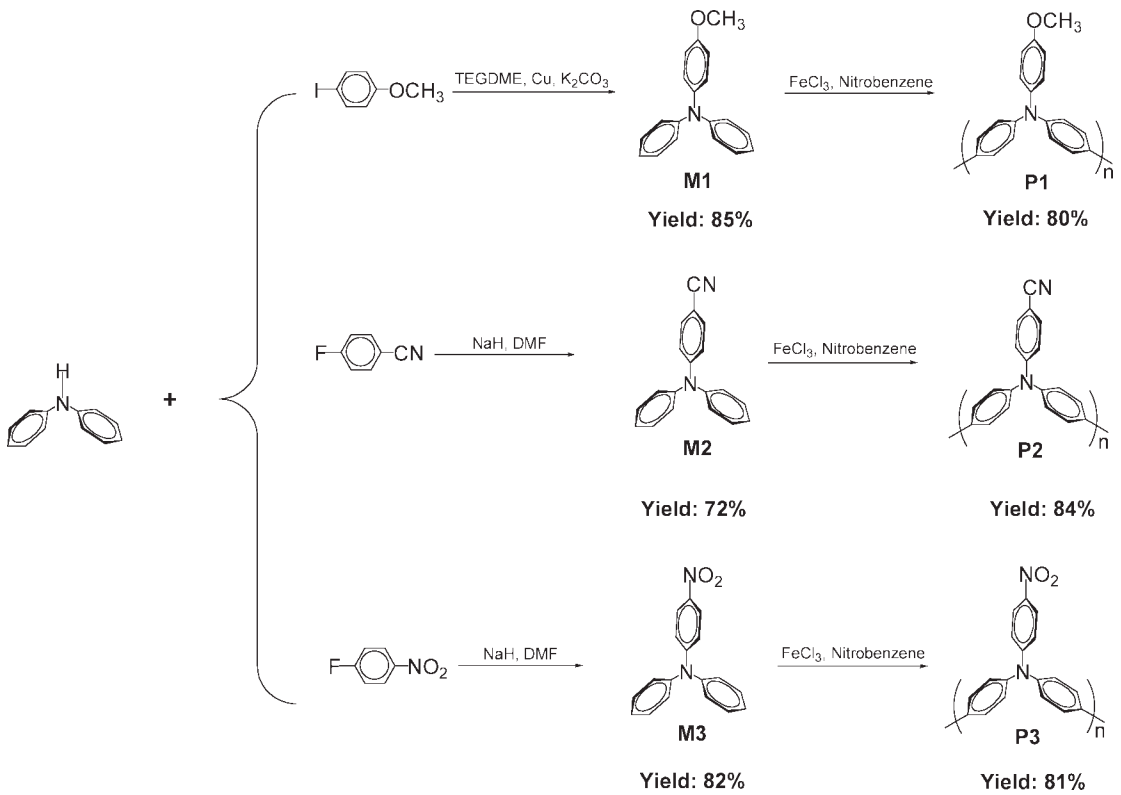

Scheme 1. Synthesis routes for monomers and polymers.

synthesized by the reaction of diphenylamine with 4-iodoanisole. **M3** (Mp: 144–145 °C) was prepared by the aromatic nucleophilic amination of 4-fluoronitrobenzene and diphenylamine in DMF in the presence of sodium hydride.

4-Cyanotriphenylamine (M2)

A mixture of 1.07 g (45 mmol) of sodium hydride and 100 mL of DMF was stirred at room temperature. To the mixture, 6.77 g (40 mmol) of diphenylamine and 4.97 g (41 mmol) of 4-fluorobenzonitrile were added in sequence. The mixture was heated with stirring at 140 °C for 15 h under nitrogen and then precipitated into 700 mL of ice water. The products was filtered and recrystallized from methanol to give 7.78 g (72% in yield) of pale gray needles. Mp = 128–130 °C (lit. 126–127 °C)[45] measured by differential scanning calorimeter (DSC) at 10 °C/min. FTIR (KBr): 2214 cm^{-1} (C≡N).

^{1}H NMR (DMSO-d_6, δ, ppm): 7.57 (d, J = 8.43 Hz, 2H), 7.40 (t, J = 15.33 Hz, 4H), 7.22–7.14 (m, J = 25.86 Hz, 6H), 6.82 (d, J = 8.43 Hz, 2H). ^{13}C NMR (DMSO-d_6, δ, ppm): 151.4, 145.5, 133.6, 130.2, 126.5, 125.7, 119.6, 118.7, 101.2. Anal. Calcd. for $C_{19}H_{14}N_2$ (270.33): C, 84.42%; H, 5.22%; N, 10.36%. Found: C, 84.33%; H, 5.20%; N, 10.47%.

Polymer Synthesis

Poly[N,N-diphenyl-4cyanophenylamine-4′, 4″-diyl] (P2)

In a 50-mL round-bottomed flask fitted with a three-way stopcock were placed **M2** (1.62 g, 6.0 mmol), $FeCl_3$ (2.43 g, 15.0 mmol), and nitrobenzene (12 mL) under nitrogen. The solution was stirred at room temperature for 24 h and poured into a mixture of methanol containing 10% hydrochloric acid. The precipitate was collected and washed thoroughly with aqueous ammonium hydroxide. Precipitations from chloroform into methanol were carried out twice for further purification to afford the polymer 1.35 g (84% in yield). FTIR (KBr): 2212 cm^{-1} (C≡N).

^{1}H NMR ($CDCl_3$, δ, ppm): 7.58 (d, J = 8.43 Hz, 4H), 7.49 (d, J = 8.16 Hz, 2H), 7.23 (d, J = 8.16 Hz, 4H), 7.10 (d, J = 8.43 Hz, 2H). ^{13}C NMR ($CDCl_3$, δ, ppm): 151.4, 145.5, 136.8, 133.3, 128.1, 126.1, 120.6, 119.5, 103.4. Anal. Calcd. for $(C_{19}H_{12}N_2)_n$ $(268.31)_n$: C, 85.05%; H, 4.51%; N, 10.44%. Found: C, 84.33%; H, 5.20%; N, 10.47%. The polymers (**P1** and **P3**) were prepared by the same method but the reaction time was different (**P1** for 24 h, **P3** for 18 h).

ELEM. ANAL. data of **P1**: Anal. Calcd. for $(C_{19}H_{15}NO)_n$ $(273.33)_n$: C, 83.49%; H, 5.53%; N, 5.12%. Found: C, 82.89%; H, 5.50%; N, 5.06%. ELEM. ANAL. data of **P3**: Anal. Calcd. for $(C_{18}H_{12}N_2O_2)_n$ $(288.30)_n$: C, 74.99%; H, 4.20%; N, 9.72%. Found: C, 73.43%; H, 4.65%; N, 10.13%.

Preparation of the Films

A polymer solution was made by the dissolution of about 0.7 g of the **P2** sample in 8 mL of NMP. The homogeneous solution was poured into a 9-cm glass petri dish, which was placed in a 90 °C oven overnight for the slow release of the solvent, and then the film was stripped off from the glass substrate and further dried *in vacuo* at 180 °C for 10 h. The obtained films were used for measurements of molecular weight, solubility, and thermal properties.

Measurements

Infrared spectra were recorded on a Perkin–Elmer RXI FTIR spectrometer. ELEM. ANAL. were run in an Elementar VarioEL-III. ^{1}H and ^{13}C NMR spectra were measured on a Bruker AV-300 FT-NMR system. The inherent viscosities were determined at 0.5 g/dL concentration using a Tamson TV-2000 viscometer at 30 °C. Ultraviolet–visible (UV–vis) spectra of the polymer films were recorded on a Varian Cary 50 Probe spectrometer. Gel permeation chromatography (GPC) was carried out on a Waters chromatography unit interfaced with a Waters 2414 refractive index detector. Two Waters 5 μm Styragel HR-2 and HR-4 columns (7.8 mm I. D. × 300 mm) connected in series were used with NMP as the eluent at a flow rate of 1 mL/min and were calibrated with narrow polystyrene standards. Thermogravimetric analysis (TGA) was conducted with a PerkinElmer Pyris 1 TGA. Experiments were carried out on ~6–8 mg film samples heated in flowing nitrogen or air (flow rate = 20 cm^3/min) at a heating rate of 20 °C/min. DSC analyses were performed on a PerkinElmer Pyris Diamond DSC at a scan rate of 20 °C/min in flowing nitrogen (20 cm^3/min). Thermomechanical analysis (TMA) was conducted with a PerkinElmer TMA 7 instrument. The TMA experiments were conducted from 50 to 280 °C at a scan rate of 10 °C/min with a penetration probe 1.0 mm in diameter under an

Table 1. Solubility and GPC Data

Code	η_{inh}[a]	M_w[b]	M_n[b]	PDI[c]	Solvent[d] NMP	DMAc	DMSO	DMF	THF	$CHCl_3$
P1	0.09	3,300	1,900	1.74	++	++	++	++	++	++
P2	0.19	26,200	14,400	1.82	++	++	++	+h	++	++
P3	0.48	1263,000	365,000	3.46	+h	–	–	–	–	–

[a] Measured at a polymer concentration of 0.5 g/dL in NMP at 30 °C.
[b] Average molecular weights relative to polystyrene standard in NMP by GPC.
[c] PDI = M_w/M_n.
[d] ++, soluble at room temperature; +h, soluble on heating; –, insoluble even on heating.

applied constant load of 10 mN. Cyclic voltammetry was performed with a Bioanalytical System Model CV-27 potentiostat and a BAS X-Y recorder with ITO (polymer films area about 0.7 cm ×0.5 cm) was used as a working electrode and a platinum wire as an auxiliary electrode at a scan rate of 50 mV/s against a Ag/AgCl reference electrode in solution of 0.1 M TBAP/acetonitrile (CH_3CN). Voltammograms are presented with the positive potential pointing to the left and with increasing anodic currents pointing downward. The spectroelectrochemical cell was composed of a 1 cm cuvette, ITO as a working electrode, a platinum wire as an auxiliary electrode, and an Ag/AgCl reference electrode. Absorption spectra in spectroelectochemical analysis were measured with a HP 8453 UV–visible spectrophotometer. Photoluminescence spectra were measured with a Jasco FP-6300 spectrofluorometer. Fluorescence quantum yields (Φ_F) of **P2** in different solvent were measured by using quinine sulfate in 1 N H_2SO_4 as a reference standard ($\Phi_F = 0.546$).[46] All corrected fluorescence excitation spectra were found to be equivalent to their respective absorption spectra.

RESULTS AND DISCUSSION

Monomer Synthesis

M2 and **M3** were prepared by the condensation of diphenylamine with 4-fluorobenzonitrile and 4-fluoronitrobenzene, respectively, according to the synthetic route outlined in Scheme 1. **M2** was purified by recrystallization from a methanol to give pale gray needles, which is a blue light (453 nm) emitter with photoluminescence quantum efficiency of 36%. **M3** was purified by recrystallization from an ethanol to give orange crystals. ELEM. ANAL., IR, ^{1}H NMR, and ^{13}C NMR spectroscopic techniques were used to identify chemical structures of monomers. Figure S1 illustrated the ^{1}H NMR and ^{13}C NMR spectra of **M2**. Assignments of each carbon and proton are assisted by the two-dimensional NMR spectra shown in Figures S2 and S3, which agree well with the proposed molecular structure of **M2**. The ELEM. ANAL.

Table 2. Thermal Properties

Code	T_g (°C)[a]	T_s (°C)[b]	T_d at 5% Weight Loss[c] N_2	Air	T_d at 10% Weight Loss[c] N_2	Air	Char Yield Weight (%)[d]
P1	–[e]	150	460	455	500	500	60
P2	205	196	615	610	655	630	71
P3	203	195	460	450	500	490	78

[a] Midpoint temperature of baseline shift on the DSC heating trace (rate 20 °C /min).
[b] Softening temperature measured by TMA with a constant applied load of 10 mN at a heating rate of 10 °C /min.
[c] Decomposition temperature, recorded via TGA at a heating rate of 20 °C /min and a gas-flow rate of 20 cm^3/min.
[d] Residual weight percentage at 800 °C in nitrogen.
[e] –: Nondetectable.

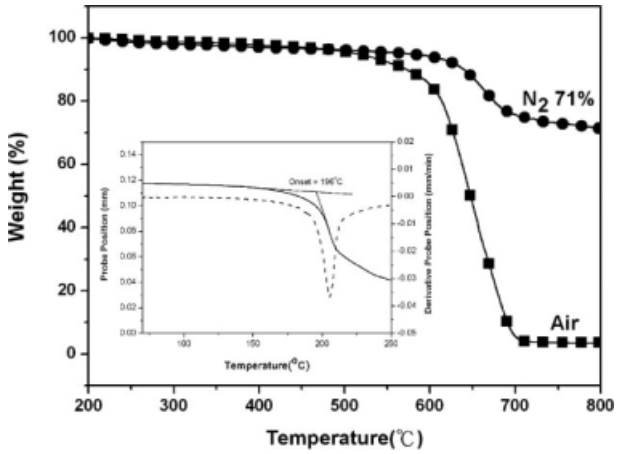

Figure 1. TGA and TMA curves of **P2** (TGA: a scan rate of 20 °C/min; TMA: heating rate = 10 °C/min; applied force = 10 mN).

on the C, H, and N also has an excellent agreement with the theoretical content. These results suggest the successful synthesis of the monomer (4-cyanotriphenylamine, **M2**).

Polymer Synthesis

P2 could be readily prepared by oxidative coupling polymerization of **M2** using $FeCl_3$ as an oxidant. The structure of polymer was confirmed by IR, ^1H and ^{13}C NMR spectroscopy shown in Figures S4 and S1, respectively. DEPT135 NMR shown in Figure S5 demonstrates that the coupling reaction occurred at para-position of the 4-cyanotriphenylamine moiety. The introduction of electron-withdrawing group can effectively increase oxidative coupling reaction rate because of the higher oxidative potential and lower electrochemical stability by electron-withdrawing substituent effect.[42] Thus, the conjugated **P2** and **P3** exhibited much higher molecular weight than the from electron-donating–substituted TPA **P1**. The inherent viscosities of the polymers **P1**–**P3** measured in NMP at 30 °C were 0.09, 0.19, and 0.48 dL/g, respectively. Figure S6 shows the molecular weight curves of **P1**–**P3** measured by GPC using polystyrenes as standard and NMP as solvent, and the weight–average molecular weights (M_w) were 3300, 26,200, and 1263,000 with polydispersity index (M_w/M_n) of 1.74, 1.82, and 3.46, respectively. The extremely high molecular weight of **P3** could be attributed to the poor cationic radical stability after oxidation of the nitro-substituted TPA structure (monomer **M3**).

Polymer Properties

Basic Characterization

P1 and **P2** showed excellent solubility in various organic solvents even less polar solvents such as chloroform and THF (Table 1), but **P3** only could dissolve in NMP with heating. The lowering solubility of **P3** could be attributed to both the extremely high molecular weight of **P3** and the much stronger acceptor substituent (—NO_2), which can enhance the intermolecular charge transfer attraction between the nitrogen atom of TPA unit and the nitro groups. The thermal properties of **P1**–**P3** were investigated with TGA, TMA, and DSC. The results are summarized in Table 2. TGA curves of **P2** in both air and nitrogen atmospheres are shown in Figure 1. These polymers exhibited good thermal stability with a 10% weight loss temperature in excess of 500 °C, and char yield at 800 °C higher than 60% in nitrogen. The high char yield of the polymer could be

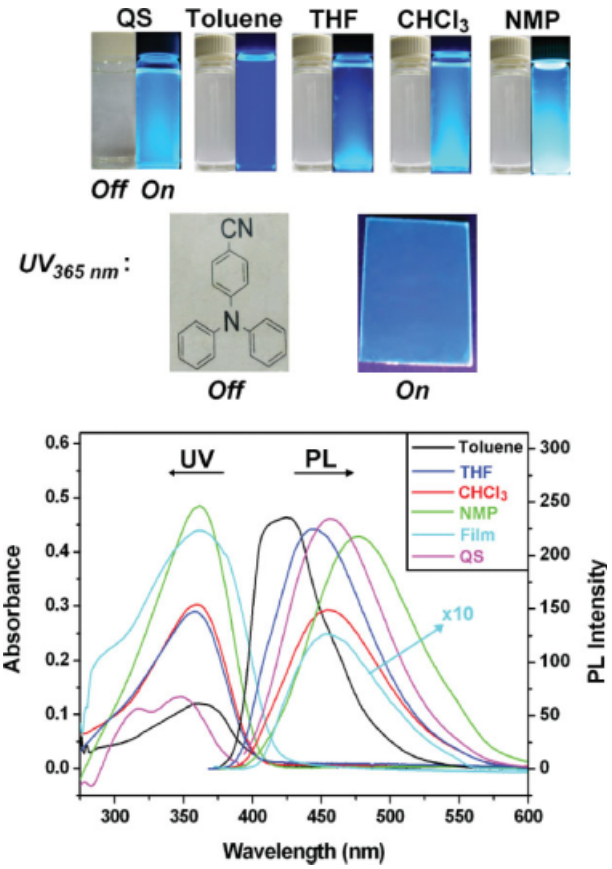

Figure 2. Molar absorptivity (left) and photoluminescence intensity (right) of **P2** in different polarity organic solvent (~1 × 10^{-5} M) and thin film.

Table 3. Optical Properties

	NMP (1×10^{-5} M) solution, r.t.			Film, r.t.			
Code	λ_{abs} (nm)	λ_{em} (nm)	Φ_F (%)[a]	λ_0[b] (nm)	λ_{abs} (nm)	λ_{onset} (nm)	λ_{em} (nm)
M1	303	435	63	–[c]	–	–	–
M2	329	453	36	–	–	–	–
M3	288,404	498	0.5	–	–	–	–
P1	370	435	51	430	371	437	446
P2	364	477	16	406	362	426	454
P3	404	492	0.1	506	336,456	575	–

[a] The value was measured by using quinine sulfate (dissolved in H_2SO_4 with a concentration of 10^{-5} M, assuming fluorescence quantum efficiency of 0.546) as a standard at 24–25 °C.
[b] The cutoff wavelengths (λ_0) from the transmission UV/vis spectra of absorption polymer films (30–60 μm).
[c] –: Nondetectable.

ascribed to their high aromatic content. The **P2** and **P3** revealed softening temperature (T_s) 196 and 195 °C determined from the onset temperature of the probe displacement on the TMA, and exhibited glass transition temperature (T_g) 205 and 203 °C by DSC trace of the polymer films.

Optical and Electrochemical Properties

The UV–vis absorption and photoluminescence spectra of **P2** were investigated in dilute solution (10^{-5} M) of different polarity organic solvents and thin film state at room temperature (Fig. 2), and the results are listed in Tables 3 and 4. The **P2** shows main absorption peak at 358–364 nm (in different solutions) and 362 nm (in film state), which is attributed to the electron transition of π–π^* along the main chain. The absorption peak wavelength is nearly solvent-polarity independent, indicating little interaction in the ground state during exciting process. From photoluminescence spectra in Figure 2, **P2** in toluene solution exhibited a maximum blue photoluminescence peak at 429 nm with photoluminescence quantum efficiency of 45% by comparing with that of quinine sulfate. When the polarity increases from toluene to NMP, the emission spectra of **P2** reveal a red shift from 429 to 477 nm.[47] The oxidation potentials of **P1**–**P3** are listed in Table 5. As the substituents vary from electron-donating (—OCH_3) to electron-withdrawing (—NO_2) groups, it could be observed that methoxy-substituted **P1** exhibited much easier to be oxidized than cyano-substituted **P2** and then nitro-substituted **P3**. Figure 3 shows the cyclic voltammograms of **M2** and **P2** with clear onset oxidation potentials E_{onset} at 1.07 and 0.99 V, respectively. The i_{pc}/i_{pa} relationship is approximately equal to 1 for **P2**, indicating that the polymer produced by the oxidative coupling reaction is stable in the time scale of a CV scan even after over 30 cyclic scans. Figure 4 shows the cyclic voltammograms of **M3** and **P3** with clear onset oxidation potential E_{onset} at 1.19 and 1.00 V, respectively, which are higher than **M2** series because of more electron-withdrawing nitro group induced. The HOMO energy levels of the polymers were determined from their oxidation onset potentials. The oxidation onset potential for **P2** has been determined as 0.99 V, and the external ferrocene/ferrocenium (Fc/Fc^+) redox standard $E_{1/2}$ is 0.46 V versus Ag/AgCl in CH_3CN. Assuming that the HOMO energy for the Fc/Fc^+ standard is 4.80 eV with respect to the zero vacuum level, the HOMO energy for **P2** was estimated to be 5.33 eV. The film onset absorption value is 426 nm and estimated optical band gap of the **P2** is around 2.91 eV. **P1** and **P3** were calculated by the same method. The cutoff wavelengths (absorption edge) from UV–vis transmittance

Table 4. Optical Properties: Solvent Effect

	(1×10^{-5} M) solution, r.t.		
P2	λ_{abs} (nm)	λ_{em} (nm)	Φ_F[a] (%)
Toluene	360	429	45
THF	358	445	25
$CHCl_3$	360	455	16
NMP	364	477	16

[a] The value was measured by using quinine sulfate (dissolved in H_2SO_4 with a concentration of 10^{-5} M, assuming fluorescence quantum efficiency of 0.546) as a standard at 24–25 °C.

Table 5. Electrochemical Properties

	Oxidation	Reduction					
Code	E_{onset}	E_{onset}	HOMO[a]	LUMO[b]	LUMO[c]	E_g^{Opt} (eV)[d]	E_g^{ECe}
M1	0.82	–	5.16	–[f]	–	–	–
M2	1.07	–	5.41	–	–	–	–
M3	1.19	−1.04	5.53	–	3.30	–	2.23
P1	0.67	–	5.01	2.17	–	2.84	–
P2	0.99	–	5.33	2.42	–	2.91	–
P3	1.00	−1.03	5.34	3.18	3.31	2.16	2.03

[a] The HOMO energy levels were calculated from cyclic voltammetry and were referenced to ferrocene (4.8 eV).
[b] LUMO = HOMO − E_g^{Opt}.
[c] LUMO = HOMO − E_g^{ECe}.
[d] The data were calculated by the equation: energy gap $E_g^{Opt} = 1240/\lambda_{onset}$.
[e] $E_g^{EC} = E_{onset}^{ox} - E_{onset}^{red}$.
[f] –: Nondetectable.

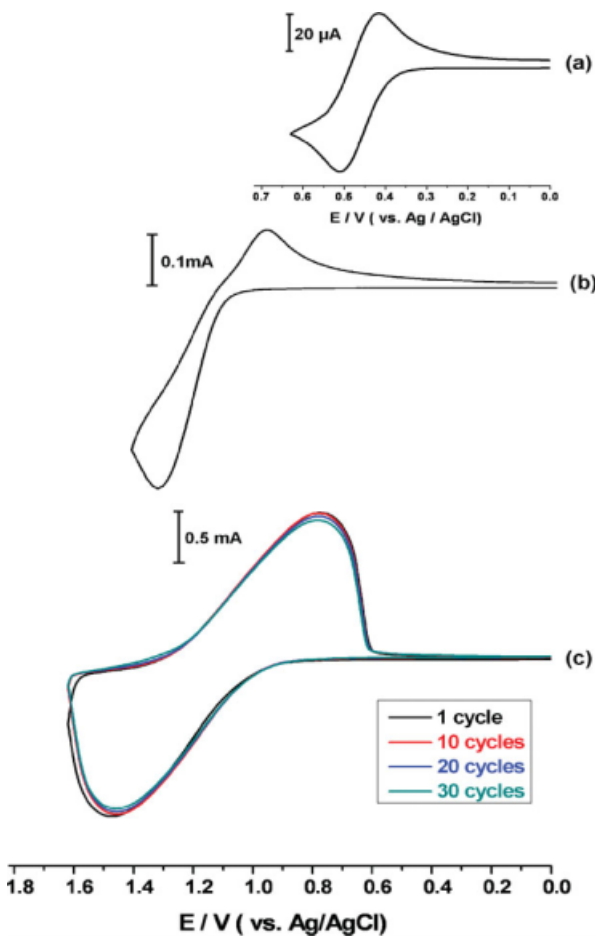

Figure 3. Cyclic voltammograms of (a) ferrocene, (b) **M2,** and (c) **P2** film onto an indium-tin oxide (ITO)-coated glass substrate in CH_3CN containing 0.1 M TBAP. Scan rate = 50 mV/s. [Color figure can be viewed in the online issue, which is available at www.interscience.wiley.com.]

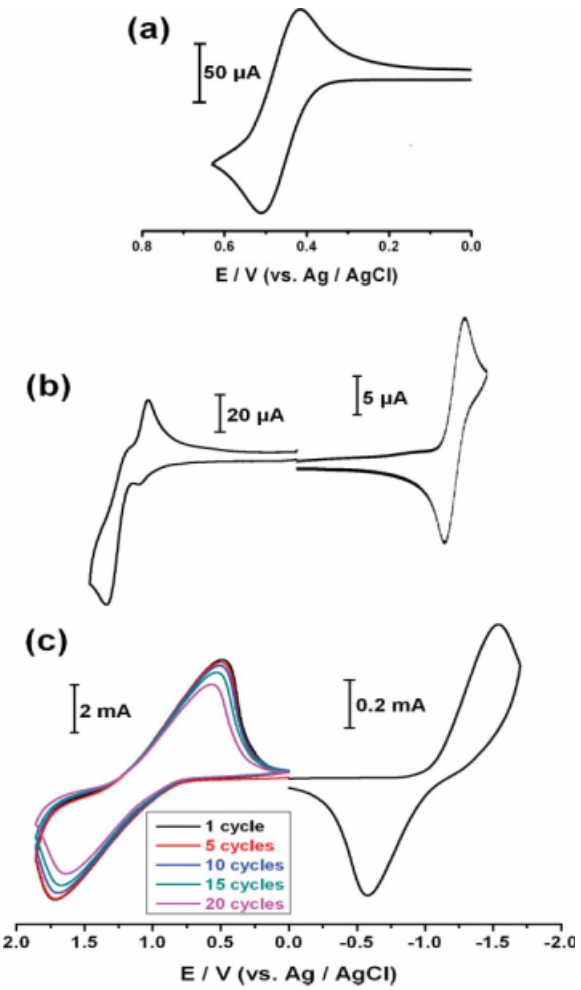

Figure 4. Cyclic voltammograms of (a) ferrocene, (b) **M3,** and (c) **P3** film onto an indium-tin oxide (ITO)-coated glass substrate in CH_3CN containing 0.1 M TBAP. Scan rate = 50 mV/s. [Color figure can be viewed in the online issue, which is available at www.interscience.wiley.com.]

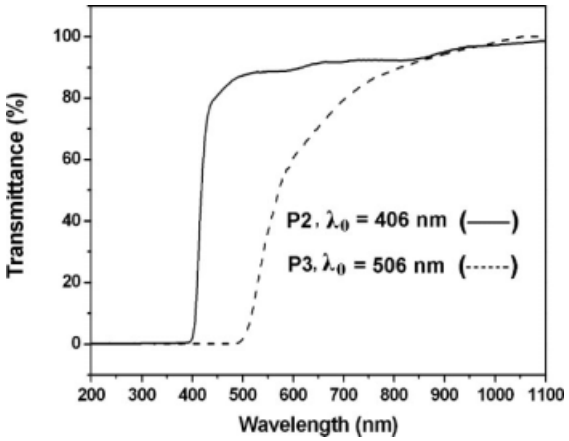

Figure 5. Transmission UV–visible absorption spectra of **P2** and **P3** films (Thin film: 30–60 μm).

spectrum were **P2** = 406 and **P3** = 506 nm (Fig. 5).

Electrochromic Characteristics

Anodically electrochromic materials could exhibit different colors depending on their oxidation state. The applications for electrochromic-conjugated polymers are quite diverse because of several favorable properties of these materials. Because the conjugated polymers at various oxidation states are quite stable, the colors corresponding to these states are long-lasting. In addition, conjugated polymeric electrochromics usually show fast switching times and exhibit color changes upon lower applying potentials.[48–51]

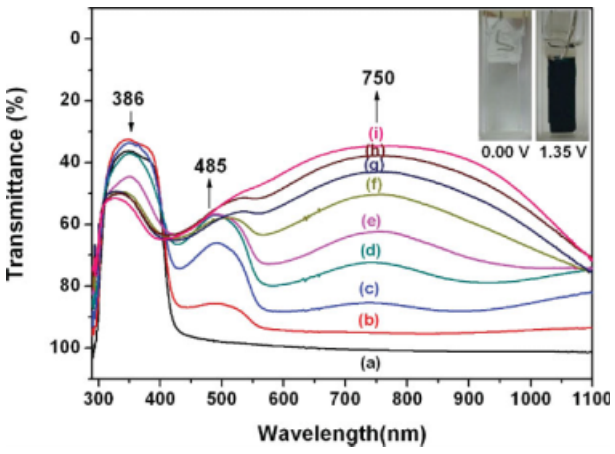

Figure 6. Electrochromic behavior of **P2** thin film (in CH_3CN with 0.1 M TBAP as the supporting electrolyte) at (a) 0.00, (b) 1.00, (c) 1.05, (d) 1.10, (e) 1.15, (f) 1.20, (g) 1.25, (h) 1.30, and (i) 1.35 V. [Color figure can be viewed in the online issue, which is available at www.interscience.wiley.com.]

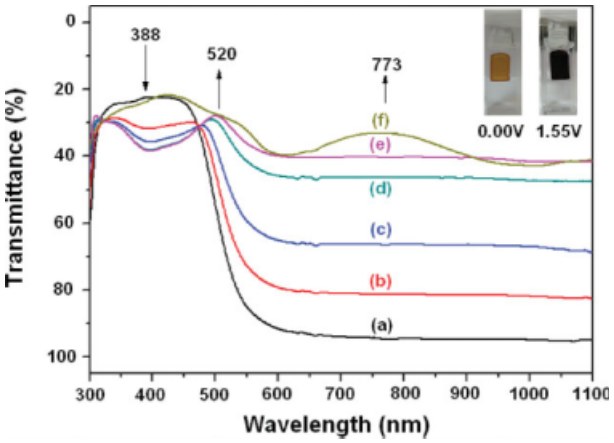

Figure 7. Electrochromic behavior of **P3** thin film (in CH_3CN with 0.1 M TBAP as the supporting electrolyte) at (a) 0.00, (b) 1.10, (c) 1.20, (d) 1.35, (e) 1.45, and (f) 1.55 V. [Color figure can be viewed in the online issue, which is available at www.interscience.wiley.com.]

Spectroelectrochemical analysis of the **P2** and **P3** films was carried out on an ITO-coated glass substrate by stepping the potential between 0.00 $\rightleftarrows$ 1.35 and 0.00 $\rightleftarrows$ 1.55 V, respectively. The transmittance (% T) at 386, 485, and 750 nm was monitored for **P2** as shown in Figure 6, and peaks showed at 388, 520, and 773 nm for **P3** in Figure 7. When the applied potentials increased positively from 0.00 to 1.35 V, the peak of absorption at 386 nm, characteristic for neutral state **P2** decreased gradually while new bands grew up at 485 and 750 nm because of the oxidation of TPA moiety. The new spectrum was assigned as that of

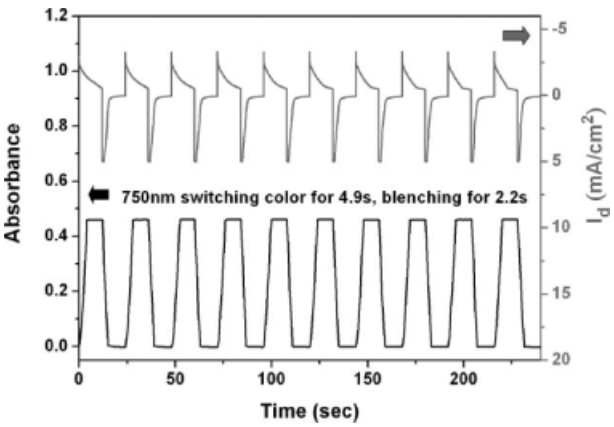

Figure 8. Potential step absorptometry and current consumption of **P2** (in CH_3CN with 0.1 M TBAP as the supporting electrolyte) by applying a potential step (0.00 V $\rightleftarrows$ 1.35 V), (coated area: 1 cm^2), and cycle time 24 s.

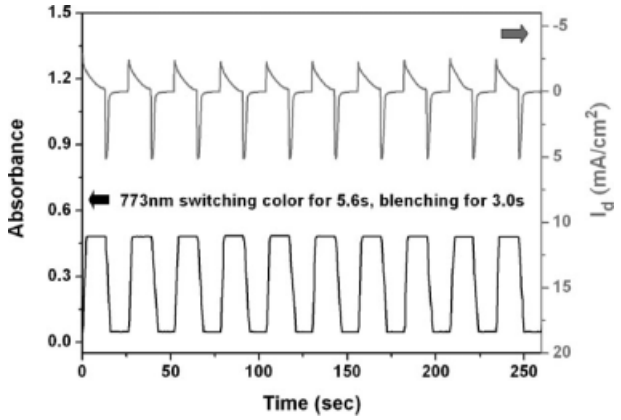

Figure 9. Potential step absorptometry and current consumption of **P3** (in CH_3CN with 0.1 M TBAP as the supporting electrolyte) by applying a potential step (0.00 V $\rightleftarrows$ 1.55 V), (coated area: 1 cm^2), and cycle time 26 s.

the stable cationic radical $\mathbf{P2}^+$, and the film color changed from original colorless to blue with high contrast of optical transmittance change (ΔT %) up to 62% at 750 nm. For **P3** film, color changed from original orange to deep blue or near black with high contrast of optical transmittance change (ΔT %) up to 61% at 773 nm.

The stability and response time upon electrochromic switching of the polymer film **P2** between neutral and oxidized forms with time intervals of 24 s are shown in Figure 8, and absorbance at 386, 485, and 750 nm was monitored versus time. The switching time was defined as the time required for reach 90% of the full change in absorbance after the switching of the potential. For most electrochromic films, the oxidation (coloration step) of the neutral form proceeded more slowly than the reduction (bleaching step) of the oxidized form because of the difference in charge-transport rates between the two forms.[52–55] **P2** film required 4.9 s at 1.35 V for switching color and 2.2 s for bleaching, and **P3** required 5.6 s at 1.55 V for switching color and 3.3 s for bleaching (Fig. 9). The amount of charge (Q) in each current curve for both processes was very similar that reveals the stable anodic electrochemical characteristic of **P2** and **P3** film. The value of the charge was used to calculate the coloration efficiency (η) by the equation[56] $\eta = \Delta A\ (\lambda)/Q$, where Q is the injected charge per unit electrode area (C/cm^2) and ΔA is the change in absorbance during a redox step. The **P2** coloration efficiency at 750 nm is as high as about 215 cm^2/C with high absorbance change (ΔA) up to 0.46. After over continuous 10 cyclic switches between 0.00 and 1.35 V, the polymer films still exhibited excellent stability of electrochromic characteristics. The **P3** coloration efficiency at 773 nm is as high as about 260 cm^2/C.

CONCLUSIONS

Poly(triphenylamine)s having high molecular weight were successfully synthesized from 4-cyanotriphenylamine and 4-nitrotriphenylamine by oxidative coupling polymerization using $FeCl_3$ as an oxidant. These results presented herein also demonstrated that incorporating electron-withdrawing substituents at para-position of TPA not only could increase the molecular weight of the poly(triphenylamine)s while maintaining good thermal stability but also revealed adjustable band gaps, good electrochemical stability, and highly electrochromic contrast characteristics. Thus, these polymers could be good candidates as electrochromic and electroactive materials because of their proper HOMO value, excellent thermal stability, and reversible electrochemical behavior.

REFERENCES AND NOTES

1. Heeger, A. J. Solid State Commun 1998, 107, 673–679.
2. Yin, S. G.; Wang, Z. J.; Yang, X. H.; Huang, X. R.; Zhang, F. G.; Xu, X. R. J Appl Polym Sci 1999, 74, 3535–3540.
3. Kietzke, T.; Neher, D.; Landfester, K.; Montenegro, R.; Güntner, R.; Scherf, U. Nat Mater 2003, 2, 408–412.
4. Tao, X. T.; Zhang, Y. D.; Wada, T.; Sasabe, H.; Suzuki, H.; Watanabe, T.; Miyata, S. Adv Mater 1998, 10, 226–230.
5. Akcelrud, L. Prog Polym Sci 2003, 28, 875–962.
6. Tang, C. W.; VanSlyke, S. A. Appl Phys Lett 1987, 51, 913–915.
7. Yu, W. L.; Pei, J.; Huang, W.; Heeger, A. J. Chem Commun 2000, 681–682.
8. Pei, Q.; Yang, Y. Chem Mater 1995, 7, 1568–1575.
9. Tang, C. W.; VanSlyke, S. A.; Chen, C. H. J Appl Phys 1989, 85, 3610–3616.
10. Adachi, C.; Nagai, K.; Tamoto, N. Appl Phys Lett 1995, 66, 2679–2681.
11. Shirota, Y. J Mater Chem 2000, 10, 1–25.
12. Shirota, Y. J Mater Chem 2005, 15, 75–93.
13. Seo, E. T.; Nelson, R. F.; Fritsch, J. M.; Marcoux, L. S.; Leedy, D. W.; Adams, R. N. J Am Chem Soc 1966, 88, 3498–3503.

14. Ito, A.; Ino, H.; Tanaka, K.; Kanemoto, K.; Kato, T. J Org Chem 2002, 67, 491–498.
15. Son, J. M.; Mori, T.; Ogino, K.; Sato, H.; Ito, Y. Macromolecules 1999, 32, 4849–4854.
16. Wang, K.-L.; Tseng, T.-Y.; Tsai, H.-L.; Wu, S.-C. J Polym Sci Part A: Polym Chem 2008, 46, 6861–6871.
17. Park, M. H.; Huh, J. O.; Do, Y.; Lee, M. H. J Polym Sci Part A: Polym Chem 2008, 46, 5816–5825.
18. Vellis, P. D.; Mikroyannidis, J. A.; Cho, M. J.; Choi, D. H. J Polym Sci Part A: Polym Chem 2008, 46, 5592–5603.
19. Huo, L.; Tan, Z.; Wang, X.; Zhou, Y.; Han, M.; Li, Y. J Polym Sci Part A: Polym Chem 2008, 46, 4038–4049.
20. Li, Y.; Xue, L.; Xia, H.; Xu, B.; Wen, S.; Tian, W. J Polym Sci Part A: Polym Chem 2008, 46, 3970–3984.
21. Karastatiris, P.; Mikroyannidis, J. A.; Spiliopoulos, I. K. J Polym Sci Part A: Polym Chem 2008, 46, 2367–2378.
22. Liou, G.-S.; Lin, H.-Y.; Hsieh, Y.-L.; Yang, Y.-L. J Polym Sci Part A: Polym Chem 2008, 45, 4921–4932.
23. Kuo, C.-H.; Cheng, W.-K.; Lin, K.-R.; Leung, M.-K.; Hsieh, K.-H. J Polym Sci Part A: Polym Chem 2008, 45, 4504–4513.
24. Ogino, K.; Kanegae, A.; Yamaguchi, R.; Sato, H.; Kurjata, J. Macromol Rapid Commun 1999, 20, 103–106.
25. Wu, A.; Kakimoto, M. Adv Mater 1994, 7, 812–814.
26. Nishikata, Y.; Fukui, S.; Kakimoto, M.; Imai, Y.; Nishiyama, K.; Fujihira, M. Thin Solid Films 1992, 210/211, 296–298.
27. Wu, A.; Jikei, M.; Kakimoto, M.; Imai, Y.; Ukishima, Y. S.; Takahashi, Y. Chem Lett 1994, 2319–2322.
28. Liou, G. S.; Hsiao, S. H.; Huang, N. K.; Yang, Y. L. Macromolecules 2006, 39, 5337–5346.
29. Cheng, S. H.; Hsiao, S. H.; Su, T. H.; Liou, G. S. Macromolecules 2005, 38, 307–316.
30. Liou, G. S.; Yang, Y. L.; Su, Y. O. J Polym Sci Part A: Polym Chem 2006, 44, 2587–2603.
31. Liou, G. S.; Huang, N. K.; Yang, Y. L. J Polym Sci Part A: Polym Chem 2006, 44, 4095–4107.
32. Liou, G. S.; Hsiao, S. H.; Chen, H. W.; Yen, H. J. J Polym Sci Part A: Polym Chem 2006, 44, 4108–4121.
33. Cheng, S. H.; Hsiao, S. H.; Su, T. H.; Liou, G. S. Polymer 2005, 46, 5939–5948.
34. Liou, G. S.; Chang, C. W. Macromolecules 2008, 41, 1667–1674.
35. Chang, C. W.; Liou, G. S. Org Electron 2007, 8, 662–672.
36. Schmitz, C.; Thelakkat, M.; Schmidt, H. W. Adv Mater 1999, 11, 821–826.
37. Goodson, F. E.; Hauck, S. I.; Hartwig, J. F. J Am Chem Soc 1999, 121, 7527–7539.
38. Lim, E.; Kim, Y. M.; Lee, J. I.; Jung, B. J.; Cho, N. S.; Lee, J.; Do, L. M.; Shim, H. K. J Polym Sci Part A: Polym Chem 2006, 44, 4709–4721.
39. Lee, S. K.; Ahn, T.; Cho, N. S.; Lee, J. I.; Jung, Y. K.; Lee, J.; Shim, H. K. J Polym Sci Part A: Polym Chem 2007, 45, 1199–1209.
40. Tanaka, S.; Iso, T.; Doke, Y. Chem Commun 1997, 2063–2064.
41. Kido, J.; Hamada, G.; Nagai, K. Polym Adv Technol 1996, 7, 31–34.
42. Nelson, R. F.; Adams, R. N. J Am Chem Soc 1968, 90, 3925–3930.
43. Liou, G. S.; Yang, Y. L.; Chen, W. C.; Su, Y. O. J Polym Sci Part A: Polym Chem 2007, 45, 3292–3302.
44. Su, T. H.; Hsiao, S. H.; Liou, G. S. J Polym Sci Part A: Polym Chem 2005, 43, 2085–2098.
45. Creason, S. C.; Wheeler, J.; Nelson, R. F. J Org Chem 1972, 37, 4440–4446.
46. Demas, J. N.; Crosby, G. A. J Phys Chem 1971, 75, 991–1024.
47. Zheng, M.; Bai, F.; Li, Y.; Yu, G.; Zhu, D. J Polym Sci Part A: Polym Chem 1999, 37, 2587–2594.
48. Sonmez, G. Chem Commun 2005, 5251–5259.
49. Sonmez, G.; Shen, C. K. F.; Rubin, Y.; Wudl, F. Angew Chem Int Ed 2004, 43, 1498–1502.
50. Sonmez, G.; Sonmez, H. B.; Shen, C. K. F.; Wudl, F. Adv Mater 2004, 16, 1905–1908.
51. Sonmez, G.; Wudl, F. J Mater Chem 2005, 15, 20–22.
52. Panero, S.; Scrosati, B.; Baret, M.; Cecchini, B.; Masetti, E. Sol Energy Mater Sol Cells 1995, 39, 239–246.
53. Sapp, S. A.; Sotzing, G. A.; Reynolds, J. R. Chem Mater 1998, 10, 2101–2108.
54. De Paoli, M. A.; Zanelli, A.; Mastragostino, M.; Rocco, A. M. J Electroanal Chem 1997, 435, 217–224.
55. Fungo, F.; Jenekhe, S. A.; Bard, A. J. Chem Mater 2003, 15, 1264–1272.
56. Monk, P. M. S.; Mortimer, R. J.; Rosseinsky, D. R. Electrochromism: Fundamentals and Applications; VCH: Weinheim, Germany, 1995.